Nanoglasses: Solids with Exceptional - Heisenberg Effect related - Spin Quantum Numbers of Itinerant Electrons

M. Ghafari and H. Gleiter
Herbert Gleiter Institute of Nanoscience, School of Materials Science &
Engineering, Nanjing University of Science and Technology, Nanjing 210094, China
ghafarijorabi@gmail.com

Abstract

This report focuses on the effects based on the indistinguishability principle of Quantum Mechanics on magnetic properties of nanoglasses. The indistinguishability principle as suggested by the Heisenberg Effect is based on quantum physical processes and the wave structure of atoms. As a result of the indistinguishability principle a chemical binding force between neighboring atoms of transition metals such as body centered iron results two initially separate itinerant electrons are joined together inside of an interfaces and generate - under certain physical conditions – an electron pair with a spin magnetic quantum number $\mu_{s.} = 1/2\mu_{B.}$ a unit with a magnetic quantum number, $\mu_{s} \approx 1 \mu_{B}$. The magnetic quantum number, $\mu_{s} \approx 1 \mu_{B}$ is established as triplet state, because in presence of spin-orbit interaction, the energy state of electrons split in three energy levels. The parallel coupling of two electrons inside of an interface arises from itinerant electrons of neighboring grains which have been magnetized in an external field of 2T. In order to evaluate the additional binding force between such atoms, the emitted γ -rays of the magnetic hyperfine field of ⁵⁷Fe has been analyzed by Mössbauer Spectroscopy. This evaluation confirms that in the case of an overlap between y-rays of atoms, the chemical binding increases. In fact it can be shown that the distance between overlapping electron orbits of atoms determines the chemical binding. The chemical binding between adjacent atoms has its highest values at lowest interatomic spacing.

Key Word and Phrases

Indistinguishability Principle, Heisenberg Materials, bcc-Fe

1. Application of the Indistinguishability Principle in Nanomaterials

Under certain physical circumstances that will be discussed in this paper it seems possible to bond together two separate itinerant electrons with a spin magnetic quantum number $\mu_s = 1/2\mu_B$ as one electron wave packet with a magnetic quantum number, $\mu_s \approx 1 \mu_B$. The magnetic quantum number, $\mu_s \approx 1 \mu_B$ is established as triplet state, because in presence of spin-orbit interaction, the energy state of electrons split in three energy levels [1]. The parallel coupling of two itinerant electrons inside of interfaces arises from the electron transfer of electrons from neighboring grains which have been magnetized in an external field of 2T. According to the experimental, the triple state is energetically the most favored state [1]. Corresponding to the quantum mechanical rules [2], [3], if an itinerant electron, e₁, from the grain, 1, and the second electron, e₂, from neighboring grain, 2, join at the same time inside of the interface, it is impossible to distinguish the two parallel electrons from each other. In other words, it is not possible to indicate which electron is coming from grain 1 and which electron is originated from grain 2. The consequence of this situation (called indistinguishability and first applied by Heisenberg) is that it creates, according to ref. 3, a chemical binding between the two electrons. This process is in classic physics unconceivable. In this paper we present evidence for the existence of indistinguishability in nanomaterials. Suppose free electrons move from a source - one electron after another - with a constant velocity straight towards a screen at a distance L. In classic physics one would expect, that all electrons hit the screen at the same position. In systems for which quantum mechanical principles apply, the experiments show, however, that the tracks of the electrons are distributed everywhere on the screen. This result indicates that the observed effects have to be explained in

the framework of the physical laws and rules of quantum mechanics. The laws of quantum mechanics indicate that the observed effects are due to the following two processes [1]-[3]:

- 1- The Uncertainly principle: $\Delta(x) \Delta(p) \ge \frac{\hbar}{4\pi}$
- 2 -The Indistinguishability Principle

The uncertainly principle specifies that it is impossible to determine the momentum of a particle, P, and its location, X, at the same time. The key reason for the spread of the random distribution of the tracks of particles is a quantum physical process classified as "Indistinguishability Principle".

The Indistinguishability Principle joins the two separated spins of 2 particles to one state and introduces an additional chemical binding between them. The experimental facts shows that inside of interfaces, the spins of the two wandering electrons have a high probability to be united and thus form a triple state. The triple state is confirmed by an internal magnetic hyperfine field [1]-[5]. The physical reason for the formation of the triple state inside of an interface is that it results in a structure of lowest energy of the systems [5], [6], because the energy states of two itinerant electrons at different energy levels will be minimalized, if two itinerant electrons adjust themself in one unit with parallel orientation of both spins in the form of a "triple state" [5]-[6]. In this triple state, the electrons/spins are indistinguishable. Hence, it is impossible to differentiate the two electrons from each other [5]. As a consequence of this Indistinguishable principle - as pioneered by Heisenberg - a chemical force, A, arises between the two electrons inside the interface. If the Coulomb interaction, $C\sim1/r$, between two electrons is included in the binding energy, A, the resulting interaction $A_{res} = A+C$ shows an exponential decrease as a function of the distance between the two electrons, (Figure 1 in ref. [2]).

The measured magnetic moment of bcc-Fe is the difference between spin densities of spin up and spin down, $\rho \uparrow (r) - \rho \downarrow (r)$. As was pointed out in ref [6], the spin density, $\rho \uparrow (r) - \rho \downarrow (r)$, is strongly localized around the atoms with a small negative value of itinerant moments between the atoms. Magnetic Compton scattering [4] and Mossbauer hyperfine field measurements scattering [5] confirmed that The macroscopically measured magnetic moment (for example by SQUID) per Fe-atom, μ_{Fe} , is the sum of the bcc-Fe 3d spins, localized around the atom, $\mu_{\text{local}} = 2.57 \mu B$, and a negative magnetic moment distributed between the Fe atoms $\mu_{\text{timerant}} = -0.4 \mu_B$ [4,5]:

$$\mu_{\text{Fe}} = \mu_{\text{local}} - \mu_{\text{itinerant}} = 2.57 \mu_{B} - 0.4 \mu_{B} = 2.17 \mu_{B}$$

The spontaneous magnetization below a specific temperature is called Curie temperature. The physical explanation of ferromagnetic state is based on two Models [7]: (1) mean field localized theory, and (2) magnetic band theory. The development of the mean field theory is based on the fundamental finding of Curie in the year 1895, which is described in ref. [7],[8]. In fact, Curie has shown that the mass susceptibility of paramagnetic materials, χ_p , as a function temperature varied inversely, $\chi_p = c/T$. Above the transition temperature, T_C , the ferromagnetic materials obey a comparable law of the form: $\chi_f = c/(T-Tc)$ known as Curie-Weiss law. Using the Boltzmann theory, Langevin [9] succeeded to explain theoretically the experimental finding of Curie for paramagnets. In this picture, a ferromagnet was considered as a paramagnet with a substantial internal magnetic field. In the year 1907 Weiss [10] proposed the existence of an internal molecular field, H_i in the order of about 100 times the saturation magnetization, M_S , $H_i = 100 M_S$. The Weiss model does not provide an understanding of why a "molecular field" exist and what is the cause for this "molecular field". Relating the ferromagnetic state to an extensive internal magnetic field was the key insight as it provided the idea of the exchange interaction between spins by Heisenberg [11] in 1928 for the understanding of the origin of the internal field of the ferromagnetic state which is related to H_i. As suggested by Heisenberg, the exchange interaction has its origin in the indistinguishability of eigenfunctions in an electron system, in which the

energy eigenvalues of spins of electrons are either parallel or antiparallel relative to the energy of the system without spins degenerated, E_0 . In fact, it was Heisenberg who has pointed out that in the ferromagnetic metals, the parallel coupling of spins relative to each other results of the minimum energy of the system. In terms of the molecular field theory, the following features of magnetization are explained by the means of the Brillouin function [12] consisting of:

- (a) The temperature dependence of magnetization, M(T), of ferromagnets
- (b) The transition temperature, T_C, from ferromagnet to paramagnet
- (c) The paramagnet susceptibility above T_C (known as Curie-Weiss low) and
- (d) The Critical behavior at temperatures close by phase transition Tc.

In addition to the local theory of magnetism - as mentioned above - a second theory named "Band magnetism" describes the ferromagnetic properties. According to the theory of Stoner [6], [12], metals containing a narrow band and a large density of states at the Fermi level with spin up and spin down, exhibit a susceptibility, $\chi_f = c/(T - Tc)$, which is large enough to split the electron band in spin up and spin down states in order to reduce the internal energy, $\Delta E < 0$. The splitting of the band [13] will inevitably lead to a ferromagnetic state if the following condition is met: $(I_0) * f(E_f) > 1$, where I_0 and $f(E_f)$ are the inter atomic exchange integral and density of state at the Fermi level. The physical reason for split of band structure in spin up and spin down state is the Pauli exclusion principal. Electrons with the opposite spin directions are able to find themselves at the same time in the same place. This leads to a strong expulsion between 3d-electrons. Moving the electrons near the Fermi surface into a higher energy state of spin down will reduce the energy of the system because the expulsion of electrons is decreased. In terms of this structural model, the measured μ_{Fe} is the sum of non-zero polarized 3d electrons with localized 3d-character as well as magnetic moment of delocalized electrons with sp- character μ_{3d} , and μ_{sp} . The electrons with sp character are distributed between atoms [6], [14]. According to theoretical band calculations are the residence probability of 3d-electrons of transition metals such as Fe, Co with spin-up and spin down concentrated around the atoms [14]. Magnetic moments, μ_{sp} with opposite spins orientations to the 3d-moments, μ_{3d} , are spread between atoms [6], [14]. The μ_{sp} arises from the hybridization of delocalized sp electrons [6], [14]. Because of the opposite spin orientation of the 3d-moments, μ_{3d} , to sp-moments, μ_{sp} , is the measured magnetic moment, μ_{Fe} , of Fe given by: $\mu_{Fe} = \mu_{3d} - \mu_{sp}$. The magnetic moment of sp-electrons is invisible for the nucleus, because the sp-electrons are distributed between atoms [6] and have no residence probability at the nucleus. At this point, it is advisable to discuss the occurrence of the internal magnetic field at the nucleus, B_{hf} , measured by nuclear methods such as the Mössbauer-effect. B_{hf} is the consequence of interaction between localized 3d-moments, μ_{3d} , with the nucleus dipole moment. On the other hand, the measured value of the measured μ_{Fe} is the sum of μ_{3d} and μ_{sp} .

Two years after the discovery of the recoil free nuclear resonance, named "Mössbauer effect", Hanna et al. [15] succeeded to measure the magnetic hyperfine field of metallic iron at room temperature to be $B_{hf}(300K) = -33.1$ Tesla. Shortly thereafter, it was found [16], [17] that the dependence of the reduced magnetic hyperfine field defined as $B_{hf}(T)/B_{hf}(T\approx 0K)$ on the reduced temperature T/T_C (T_C being the Curie temperature) is equal to the reduced measured magnetization of Fe, M(T)/M(0). It was then concluded that the B_{hf} and the measured magnetic moment of Fe, μ_{Fe} , are proportional to each other. Confirmation of such a proportionality has been suggested by several theoretical approaches [16]-[21]. From experimental results on different materials simple relationships has also been concluded. Examples are: (1) A quadratic variation of measured moment of μ^2_{Fe} as a function of B_{hf}/μ_{Fe} was found for amorphous as well as selected crystalline Metal-Metalloid alloys [16]-[21]. Unfortunately, it was not taken into account that the measured moment includes the magnetic moment of boron [21]. In this contribution, it will be shown that the moment which polarize the s electrons is different from measured moment. (2) In an experimental and theoretical approach Stearns [19],[20] determined the solute and host-moment of transition metals from the magnetic hyperfine fields of diluted Fe alloys. delocalized 3d magnetic moment and moments of electrons with sp character was included in the interpretation of data [19],[21] without using the true value of the local magnetic moment, μ_{3d} of

3d-electrons. The Mössbauer Effect Data Center [22] provides in its data base a rather complete list of Bibliographical information dealing with Mossbauer-effect including the relation between B_{hf} and magnetic moment, μ_{Fe} . As mentioned above, the relationship between B_{hf} and μ_{Fe} has not been extra sorted. It was always considered that the relationship $(B_{hf} \sim \mu_{Fe})$ connects a microscopic method, such as Mössbauer spectroscopy, and a macroscopic method, such as SQUID magnetometry. Without any doubt, besides the theoretical considerations between B_{hf} and μ_{Fe} the experimental value relating the microscopic and macroscopic quantities is relevant for scientific and technological aspects as it provides an easy way to determine the missing quantity. However, it has been assumed since discovery of Mössbauer-effect that only the 3d electrons contribute to the measured magnetic moment.

The most important aspects that give rise to the proportionality between B_{hf} and the magnetic moment of 3d-electrons, μ_{3d} are:

I) Core polarization effect

Fundamentally different from the special arrangement of s-electrons is the residence probability of 3d-electrons [23]. The 3d-electrons are able to polarize the electrons in the atomic shell what is called "Core polarization effect" e.g. of 57 Fe. The polarized s-electrons with a nonzero residence probability at the nucleus interact with the dipole moment of the nucleus. According to the Pauli exclusion principle, electrons with the opposite spin directions are able to find themselves at the same time in the same place. This leads to a strong expulsion between 3d-electrons and electron shells and moves the electrons with opposite spin directions to 3d-spins towards nucleus. This explains why the internal magnetic hyperfine fields have in comparison to the magnetic moment of spins a negative direction. The theoretically estimated value of internal magnetic field [24] originates from the interactions between the spin of filled core electron shells with the nucleus's dipole moment depends directly on radius of 3d-electrons and it is according to theory described by Novak et al. [23] B_{Cor} = -28.59 T.

II) Delocalized electrons

The contribution of non-localized electrons such as 4s electrons to the value of internal magnetic hyperfine field is low [23]-[26], B_{val} = -4.49T and will thus be neglected in this overview presentation.

III) Magnetic field of Central and neighboring atoms

⁵⁷Fe atoms and their neighbor's atoms generate a magnetic field through 3d electrons at nucleus. The interaction of this magnetic field with the dipole moment of nucleus, N_d , leads to an additional splitting of the excited state of ⁵⁷Fe. According to the theory [24]-[27], the contribution is for bcc-Fe around 1 to 2 Tesla which has to be added to the core polarization, B_{cor} as describe above.

V) Interactions with Orbital Moments

Interactions between orbital moments and N_d causes in general case a splitting of excited states of 57 Fe. Since the orbital moment of bcc-Fe is through crystalline fields not completely quenched [23]-[27], it contributes to the internal magnetic field of Fe, $B_{val} = +2.378$ T.

Blügel et al [24], have investigated the electronic and the hyperfine field of 3d impurities in Nickel. It was found that hyperfine field can be divided into local and transferred contributions that are related to local moment and surrounding atoms. The ab initio results of magnetic Guo et al. [25], show that B_{hf} is related to spin magnetic moment of Fe In an extensive investigation, Dubiel [26] has shown that the factor of proportionality between magnetic hyperfine field of ⁵⁷Fe and measured magnetic moment of Fe depends on the temperature, chemical composition and structure of metallic alloys. There is a legitimate concern about the universal validity of $P = B_{hf}/\mu_{Fe}$ [4]. In spite of the fact that factor of proportionality is not a universal value, the proportionality between the value of macroscopic magnetic moment of metallic iron, $\mu_{Fe} = 2.2\mu_{B}$, and the magnetic hyperfine field, $B_{hf} = -34$ Tesla, was never called into doubt. However, the view continues to prevail that the macroscopic magnetic moment, $\mu_{Fe} = 2.2\mu_{B}$, is caused by 3d-

electrons. But precisely here lies the problem, because in this reasoning the delocalized sp-moments between atoms cease to exist. Fortunately, the access to a material named nanoglass, which consists of amorphous nanograins, and interface makes unprecedented achievement for description of the discrepancy of relation between macroscopic (or measured) moment and B_{hf} . In this report, crystalline bcc-Fe, amorphous Fe-rich FeSc, FeCoSc alloys and nanoglass have been chosen to demonstrate the relationship between macroscopic and microscopic methods. It will be shown that using the correct factor of proportionality between 3d moment and B_{hf} of metallic alloys establishes a method for estimation of μ_{3d} and μ_{sp} .

2. Experimental

Alloys with the nominal composition of $Fe_{90-x}Co_xSc_{10}$ ($0 \le < x \le 90$) were synthesized by arc melting in an argon atmosphere. Amorphous Fe_{90-x}Co_xSc₁₀ alloys without separated interface regions were prepared using melt spinning with a wheel speed of 45 m/s in an argon atmosphere. The produced amorphous ribbons had a thickness of approximately 30 µm and a width of about 2 mm. As reported in Ref. [21], energy Dispersive X-ray Spectroscopy EDX (Oxford Instruments) was used for the analysis of the composition of the amorphous alloys. For analysis of the samples, a high-flux rotating anode X-ray diffractometer with a wavelength $\lambda_{\text{Mo-K}\alpha 1} = 0.7107 \,\text{Å}$ and highresolution parallel beam optics was employed to convert the X-ray diffraction data of amorphous FeCoSc alloys in Pair Distribution Functions. The detail for the analysis is report in ref. [28]. The distorted bcc structure of amorphous Fe_{90-x}Co_xSc₁₀ alloys remains as a function of composition of Co unchanged [28]. Further information on the state of Fe was obtained by means of Mössbauer spectroscopy. The resulting internal magnetic hyperfine distribution, P(B_{hf}), the average hyperfine field, B_{hf} and the standard deviation, σ at low temperature has been discussed. In ref. [29]. The analysis of amorphous Fe-rich, FeSc with references is described in ref. [29]. Magnetization measurements were obtained using a Superconducting Quantum Interface Device (SQUID). In addition to the investigations presented above, it was possible to prepare amorphous Fe_{90-x}Co_xSc₁₀ nanoparticles with X=0 and X=5 by consolidation of molten alloys in an Inert Gas (He) Condensation, IGC chamber [28]. He atoms act as nucleation sources. The so generated nanoparticles flow to a cold-finger available in the UHV chamber. The amorphous nanoparticles generated in this way had average sizes ranging from 3 to 12 nm and were consolidated at pressures of about 2.0 GPa. The resulting materials are called today nanoglasses. In nanoglasses, the amorphous nm-size glassy clusters are joint together by Glas/Glas interfaces. One purpose of producing such materials was to form alloys with high proportions of interfaces. The interface of nanoparticles shows physical properties which has not been observed before [30],[31]. In this contribution, the effect of the glass/glass interfaces on internal magnetic hyperfine field will be discussed.

3. Results and Discussion

As was mentioned above, the magnetic moment of 3d spins is not the only contribution to the macroscopically measured magnetic moment. The value of the measured magnetic moment of Fe is due to the sum of magnetic moment of 3d electrons with a value of μ_{3d} = 2.57 μ_B and ititnerant sp electrons between atoms, μ_{3d} = -0.4 μ_B . The residence probability of free 3d electron of transition metals with spin-up and spin-down is concentrated around the Fe-atoms [6]. Hence, the Magnetic Compton Scattering, MCS, method is a valuable experimental method to estimate the contribution of Fe- spins with 3d-character as well as their sp- character. The details of MCS method and analysis of the experimental data are described in [5], [14], [22], [30]. This contribution will be used later for the interpretation of the relationship between the magnetic moment and B_{hf} . Therefore, it is essential to discuss the results of the Mössbauer-data in details.

The analysis of Mössbauer- measurements are described somewhere else [22]. In order to gain comprehensive understanding of relations between B_{hf} , and the magnetic moment behavior, the

total magnetic moment with dominant 3d character and sp-character mentioned above will be described in more details in the following sections.

3.1. bcc-Fe

According to ref. [2], [3], the magnetic data of bcc- Fe are as follows: μ_{3d} = 2.57 μ_B , μ_{sp} = -0.49 μ_B ; $\mu_{total}(Fe) = \mu_{3d} + \mu_{sp} = 2.57\mu_B - 0.49\mu_B \approx 2.1\mu_B$. At a particular temperature, the macroscopic methods such as SQUID measures at a given temperature the total value of $\mu_{total}(Fe) \approx 2.1\mu_B$.

For a macroscopic method it is however impossible to separate the various contributions which is the sum of the positive 3d-moment and the negative spins with sp-character. A physically complete picture can be obtained on the basis of the accurate 3d- moment, μ_{3d} , which is according to the results of MCS [5],[14],[30] for bcc-Fe, $\mu_{3d}=2.57\mu_B$. The negative moment with sp-character is distributed between the atoms with no residence probability at nucleus. As a result of the interaction between the moments $\mu_{3d}=2.57\mu_B$, and the Dipole moment of the nucleus a magnetic hyperfine field results, which is described in the text above in sections I-V. The theoretical consideration of the interaction between the diploe moment of nucleus and magnetic moment should be focused on the realistic, accurate moment of the 2.57 μ_B and not at 2.1 μ_B . This gave rise to a correct ratio, $P=B_{hf}/\mu_{3d}=34.0T/2.57$ $\mu_B=13.2$ T/μ_B , between B_{hf} and magnetic moment. In the next paragraphs, the validity of proportionality, $P=B_{hf}/\mu_{3d}$ and its application will be discussed.

3.2. Amorphous Fe₉₀Sc₁₀ alloys and Fe₉₀Sc₁₀ nanoglasses

Using, the Mössbauer results [4], [28]-[30] and the radial distribution functions [30], RDF, it was demonstrated that amorphous $Fe_{90}Sc_{10}$ and FeCoSc alloys without interfaces as well as $F_{90}Sc_{10}$ nanoglass consist of distorted bcc clusters with average sizes of about 6 Fe-atoms [4]. The clusters are connected together without the formation of grain boundaries. inside of every cluster. So the entire structure of the material consists of the following two components: (1) In the center of the clusters are the atoms dense packed. (2) With increasing distances from the center (toward surface of the clusters) are the atoms less dense packed. The magnetic hyperfine field distribution of amorphous $Fe_{90}Sc_{10}$ alloy at low temperatures and in zero external magnetic field consists of two distributions; a low field distribution and a high field distribution [28]. According to the experimental observations, the low field components is caused by the dense packed atoms with a frustrated magnetic coupling (a mixture of ferro- and antiferromagnetic couplings [30]). The high ferromagnetic component is due to the less dense packed atoms with a greater atomic spacing are presented in [28].

 $Fe_{90}Sc_{10}$ nanoglasses were observed to show physical properties that are significantly different from the ones of the melt cooled material with the same chemical compositions. This difference results from the glass/glass interfaces between the small amorphous clusters with average sizes of about 5nm. In nanoglass, the fraction of interfaces is about 20 -40% of the amorphous nanograins, Fig.1. The atomic arrangements of amorphous nanograins and the distribution of magnetic hyperfine field are in a first approximation close to the amorphous alloys without interfaces [28], [30].

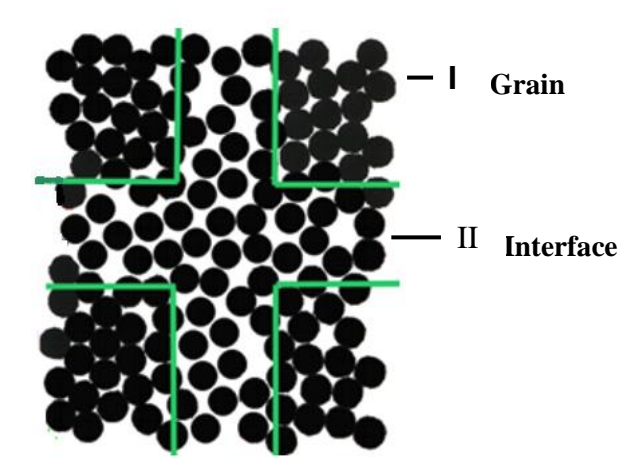


Fig.1 Atomic arrangements of nanoglass inside of the interfaces between the glassy regions and inside of the nanometer-sized glassy regions (called nanograins) of $Fe_{90}Sc_{10}$ nanoglass.

The internal magnetic hyperfine fields of interfaces and nanograins are, however, different. As presented in Fig.2, the internal magnetic hyperfine field distribution inside the nanograins of nanoglass as well as of amorphous ribbons without interfaces consists of regions with low magnetic hyperfine field distribution and regions with a high magnetic hyperfine fields.

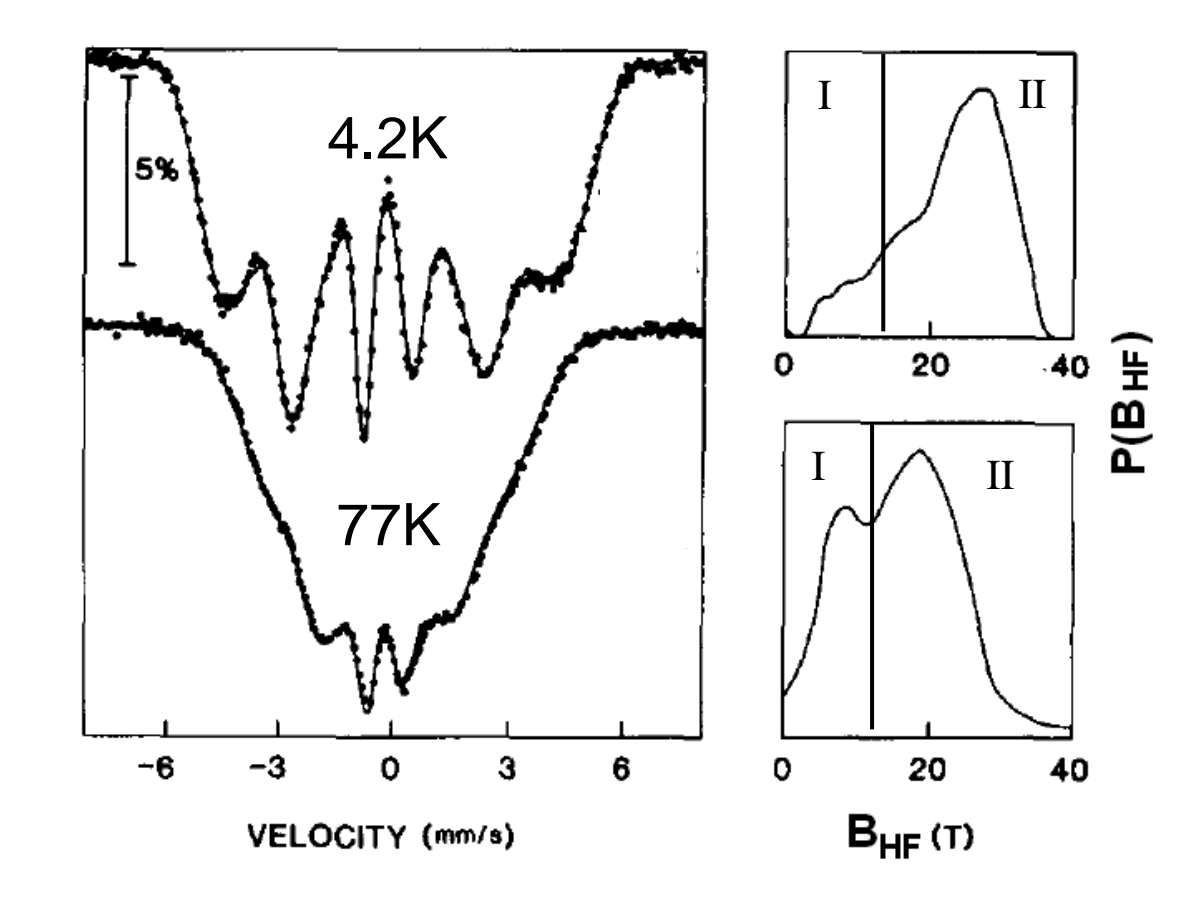


Fig.2 Mössbauer spectra and corresponding magnetic hyperfine field distributions of amorphous $Fe_{90}Sc_{10}$ ribbon at different temperature (see text).

According to the Slater-curve [7], the low and high distributions of magnetic hyperfine fields are due to the densely packed Fe-Fe areas with a negative exchange integral (region I in Fig. 2) and an antiparallel orientation of spins (region II in Fig. 2). In the specimen regions corresponding to area II of Fig.2 - the spins of the Fe-Fe atoms result in a ferromagnetic state, with a positive exchange integral. Amorphous nanoparticles with average size of about 5 nm are interconnected by interfaces. Their Mössbauer parameters are as follows [2], [3], [5]:

- (1) A magnetic hyperfine field distribution close to that of amorphous ribbon without interface.
- (2) A broad magnetic hyperfine field splitting with a maximum of about B_{hf} = 37 Tesla, which is due to the atomic arrangements at interfaces. The observed B_{hf} at interface is one of the highest magnetic hyperfine field registers in metallic Fe system.

At T<10K, the measured magnetic moment, $\mu \approx 1.67 \mu_B$, of Fe₉₀Sc₁₀ nanoglass is equal to that observed for amorphous Fe₉₀Sc₁₀ alloy without interfaces. The saturation magnetization of amorphous Fe₉₀Sc₁₀ alloy without interfaces can be reached by external fields above B_{ex} > 7Tesla. Despite of having almost the equal saturated macroscopic magnetic moment at extremely high external magnetic fields (at low temperature), µ_{Fe}≈1.67µ_B, for amorphous Fe₉₀Sc₁₀ ribbons and for Fe₉₀Sc₁₀ nanoglass) the internal magnetic field distribution for both materials different is different [2], [3] .This experimental finding suggests the question: Why - despite having the same average macroscopic moment and approximately similar atomic structures - is the Bhf(300K) of nanoglass very different from the $B_{hf}(300K)$ of the amorphous alloy (without interfaces). The answer lies in the fact that the macroscopic methods such as SQUID or PPMS measures the resulting magnetic moment which is the sum of the moments of 3d-electrons and the negative moment with sp- character. The 3d-electron of Fe₉₀Sc₁₀ nanoglass has at interface a local magnetic moment of about $\mu_{3d}\approx 2.76\mu_B$ per atom [25], which is higher than the localized 3d-band of bcc- Fe, μ_{3d} =2.57 μ_B as well as amorphous Fe₉₀Sc₁₀ alloy, μ_{3d} ≈1.8 μ_B , without interface. The consequence is a large interaction between magnetic dipole moment of nucleus and moment of 3d-electrons at interfaces, because for the Mossbauer magnetic hyperfine interaction is the itinerant moment almost invisible. These results confirm the fact that the factor of proportionality, P, between B_{hf} and magnetization is determined by μ_{3d} .

3.3. Amorphous Fe₈₅Co₅Sc₁₀ alloy and Fe₈₅Co₅Sc₁₀ nanoglass

In order to show that separation of magnetic hyperfine data is in nanoglass universally applicable, amorphous $Fe_{85}Co_5Sc_{10}$ alloy as well as nanoglass $Fe_{85}Co_5Sc_{10}$ have been investigated. Both alloy systems have equal macroscopic magnetic moment, $\mu_{measured}=1.76\mu_B$. The experimental observation has shown that the form of Mössbauer- spectra of nanoglass $Fe_{90}Sc_{10}$ is similar to that of $Fe_{85}Co_5Sc_{10}$ nanoglass.

As presented in ref. [27] the internal magnetic hyperfine field distributions of amorphous $Fe_{85}Co_5Sc_{10}$ alloy as well as $Fe_{85}Co_5Sc_{10}$ nanoglass are, however, different. In addition to a hyperfine distribution similar to amorphous alloy without interface, nanoglass has a broad hyperfine filed with an average value of about $B_{hf} \approx 37$ Tesla. This hyperfine field , $B_{hf} \approx 37$ Tesla, is due to interaction of dipole moment and 3d magnetic moment with 3d-character at interfaces. Using the relation $P=12.8=B_{hf}/\mu_{3d}$ leads to a $\mu_{3d}\approx 2.9\mu_B$. This demonstrates that it is possible to study the individual magnetic components such as μ_{3d} and μ_{sp} of alloys. In the next section, the influence of Co on magnetic coupling in amorphous $(Fe_{100-x}Co_x)_{90}Sc_{10}$ alloys will be discussed.

3.4. Amorphous (Fe_{100-x}Co_x)₉₀Sc₁₀ alloys

At T= 10 K, Mössbauer spectra together with magnetic hyperfine distributions, $P(B_{hf})$, in the range $0 \le X \le 16.5$ are presented in ref. [27]. It is worth noting that the rise in Co concentration yield a decrease of standard deviation of $P(B_{hf})$ and an increase of average B_{hf} . At low Co concentrations are various of Fe atoms in the region of dense packed clusters and magnetically

disordered. In these regions, the spins experience ferromagnetic as well as antiferromagnetic coupling . The resulting $P(B_{hf})$ is accompanied by a low magnetic hyperfine field distribution as a result of mixed magnetic interactions. An increase of cobalt concentration in the amorphous FeCoSc system is associated with a reduction of the low magnetic hyperfine field component of $P(B_{hf})$ [28]. This indicates that the increase of cobalt in amorphous $(Fe_{100-x}Co_x)_{90}Sc_{10}$ alloys causes increasingly ferromagnetic coupling. Furthermore, the decrease of standard deviation of $P(B_{hf})$ with increasing Co concentrations is another indication of ferromagnetic coupling. Similar to crystalline $Fe_{100-x}Co_x$ alloys, the increase of Co atoms from X>0 to X<20 causes an increase of the magnetic hyperfine fields. At X<11, amorphous $(Fe_{100-x}Co_x)_{90}Sc_{10}$ alloys with a distorted bcc structure [27] consists of two magnetic regions (region I with mixed interactions and region II with ferromagnetic interactions with different 3d-band structure. According to Schwartz et al. [6] the spin down state is pinned at the Fermi level. The increase of Co concentration with higher number of valence electrons per atom in comparison to Fe atoms fills only the spin up state. The result is a reduction of low magnetic hyperfine field distribution and an increase of B_{hf} .

4. Conclusions

In conclusion, the comparison of the measured B_{hf} of amorphous alloys as well as of the measured B_{hf} at the interfaces of nanoglasses with bcc-Fe indicates that the measured internal magnetic field is a consequence of the local magnetic moments based on electrons with localized 3d-character. The measured magnetic moment of Fe, μ_{Fe} , is, however, the sum of the positive moments of 3d-electrons and the negative sp moments between atoms. The measured magnetic moment is not the decisive factor for the proportionality between B_{hf} and the measured magnetic moment. The decisive factor for the proportionality is the contribution of the 3d-moments with 3d-character.

The analysis of the magnetization and internal magnetic hyperfine field results in a factor of proportionality, $P=B_{hf}/\mu_{3d}=12.8$. Fortunately, the access to materials named nanoglasses, which consists of amorphous nanograins, and interfaces between them allows us to deduce unprecedented descriptions of the discrepancy of the relation between the macroscopically measured moment and B_{hf}

In this report, crystalline bcc-Fe, amorphous Fe-rich FeSc, FeCoSc alloys and nanoglasses have been chosen to investigate and to improve our understanding of the relationship between macroscopic and microscopic methods. The results obtained so far suggest that by using the correct factors of proportionality between 3d moment and B_{hf} of metallic alloys opens the access to a new method for the estimation of μ_{3d} and μ_{sp} which reflects the structure of electrons in these materials based on the Heisenberg effect. In other words, these materials seem to open the door to a yet unexplored and perhaps also to a yet technologically unutilized family of materials.

References

- Barrow G. M., 'Die Fermi -Dirac und Bose Einsteinstatistik', Physikalische Chemie I', Bohmann-Verlag, Heidelberg Germany', 1973, 100-105.
- 2. Ghafari M., Gleiter H. and Wilde G., 'Quantum mechanical effects controlling the magnetic properties of transition metal based nanoglass', APL Quantum, 1(2024), 016103.
- 3. Ghafari M., Gleiter H. and. Feng T., 'Heisenberg indistinguishability principle versus magnetic hyperfine fields', J. Discover Nano, 20 (2025), 25-29.
- 4. Ghafari M., Hahn H. and Feng T., 'On the relationship between magnetic moment and nuclear magnetic hyperfine field of ⁵⁷Fe', Hyperfine Interact, **242** (2021), 2.
- 5. Ghafari M., Hahn H. Gleiter H., Sakurai Y, Itou M. and Kamali S., 'Evidence of itinerant magnetism in a metallic nanoglass', Appl. Phys. Lett., 101 (2012), 243104.
- 6. Schwartz K., Mohn P., Blaha P. and Kübler J., 'Electronic and magnetic structure of BCC Fe-Co alloys from band theory', J. Phys. F: Met. Phys., 14 (1984), 2659.
- 7. Cullity B.D.and Graham C. D., 'Introduction to Magnetic Materials', John Wiley & Sons, England, 2008.
- 8. Weiss P., J. Phys., 5 (1895), 289-303.

- 9. Langevin P. J., J. Chim. Phys., 5 (1905), 70 80.
- 10. Weiss P., J. Phys., 6 (1907), 661-670.
- 11. Heisenberg W., Zeitschrift für Physik', **49(9)** (1928) 619-632.
- 12. Brillouin L., J. de physique, 8(1927), 74-80.
- 13. Stoner E.C., Proc. R. Soc. Lond., A.165(922) (1938) 372-380.
- 14. Ghafari M., Sakurai Y., Peng G., Fang Y. N., Feng T., Hahn H., Gleiter H., Itou M. And Kamali S., Unexpected magnetic behavior in amorphous Co₉₀Sc₁₀ alloy', Appl. Phys. Lett., **107** (2015), 132406.
- 15. Hanna S. S., Heberle J., Littlejohn C, Perlow G. J., Preston R. S. and Vincent D. H., 'Polarized Spectra and Hyperfine Structure in ⁵⁷Fe', Phys. Rev. Lett., 4 (4) (1960), 177–180.
- 16. Hanna S.S., 'The Discovery of the Magnetic Hyperfine Interaction in the Mössbauer Effect of ⁵⁷ Fe', *In:* Gonser, U. (eds) Mössbauer Spectroscopy II. Topics in Current Physics, vol 25., Springer, Berlin, 1981.
- 17. Watson R.E. and Freeman A.J., 'Origin of Effective Fields in Magnetic Materials', Phys. Rev., 123(1961), 2027-2047.
- 18. Stearns M. B. and Wilson S. S., 'Measurements of the Conduction-Electron Spin-Density Oscillations in Ferromagnetic alloys', *Phys. Rev. Lett.*, 13 (1964), 313-315.
- 19. Overhauser A. W. and Stearns M. B., 'Spin Susceptibility of Conduction Electrons in Iron', Phys. Rev., B13 (1964), 316-324.
- 20. Lines M. E., Sol., 'Hyperfine fields in iron-metalloid ferromagnetic metals', Solid State Comm., 36 (1980), 457-460.
- 21. Stosser A., Ghafari M., Klimametov A., Gleiter H., Sakurai Y., Itou M., Kohara S., Hahn H. and Kamali S., 'Influence of interface on structure and magnetic properties of FesoBso nanoglass', J. Appl. Phys., 116(2014), 134301-07.
- 22. Mössbauer Effect Data Center: http://www.medc.dicp.ac.cn
- 23. Novak P. and Clan P., 'Contact hyperfine field at Fe nuclei from density functional Calculations', Phys. Rev., B81 (2010), 1214(1)-1214(8).
- 24. Blügel S., Akai H. A., Zeller R. and Dederich P. H, 'Hyperfine fields of 3d and 4d impurities in Nickel', *Phys. l Rev.*, **B 35** (7) (1987), 3271-3278.
- 25. Guo G. Y. and Ebert H., 'First-principles study of the magnetic hyperfine field in Fe and Co multilayers', Phys. Rev., **B53** (1996), 2492-2503.
- 26. Dubiel S. M., 'Relationship between the magnetic hyperfine field and the magnetic moment', J. of Alloys and Compounds, 488(1) (2009), 18-22.
- 27. Fang Y. N., Hahn H., S. Kobe, Witte R., Singh S. P., Feng T., and Ghafari M., Modifying the transition temperature, $120~\text{K} \le T_c \le 1150~\text{K}$, of amorphous $\text{Fe}_{90-x}\text{Co}_x\text{Sc}_{10}$ with simultaneous alteration of fluctuation of exchange integral up to zero', Scientific Reports 9, 412 (2019), 36891.
- 28. Day R. K., Dunlop J. B., Foley C. P., Ghafar M. and Park H., 'Preparation and Mössbauer study of a new Fe-rich amorphous alloy, Fe₉₀Sc₁₀', Solid State Commun., **56** (1985), 843-845.
- 29. Ghafari M., Hahn H., Gleiter H., Sakurai Y., Itou M. and Kamali S., 'Evidence of itinerant magnetism in a metallic nanoglass', Appl., 101(2012), 243104.
- 30. Ghafari M., Kohara S., Hahn H., Gleiter H., Feng T., Witte R. and Kamali S., 'Structural investigations of interfaces in Fe90Sc10 nanoglasses using high-energy x-ray diffraction', Appl. Phys. lett., 100 (2012), 13311.
- 31. Ghafari M., Gleiter H., Feng T., Ohara K. and Hahn H., 'Are Transition Metal-Rich Metallic Glasses Made Up of Distorted BCC Clusters?', J. Material Sci Eng., (2017), 6:299.